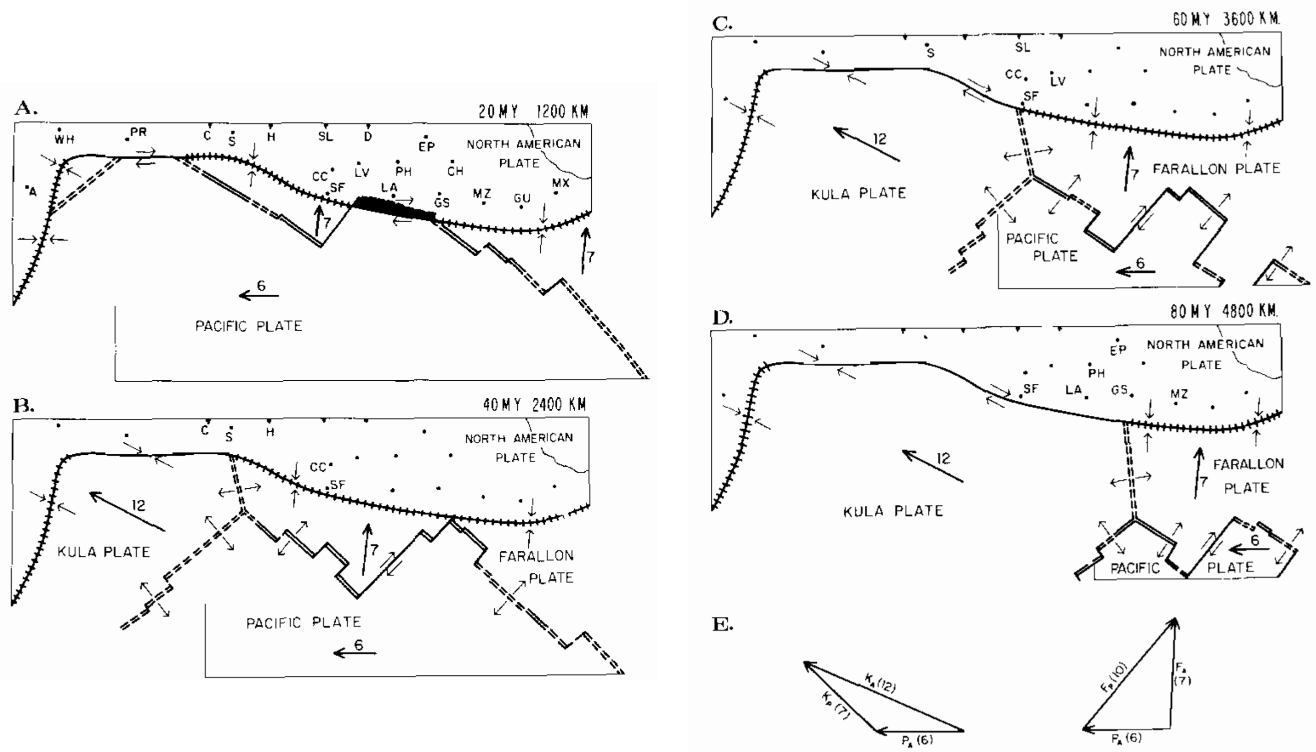

Figure 18. Plate relationships derived from extrapolation of Pacific-North American and Pacific-Kula motions through the Cenozoic. Conventions and assumptions are as in Figure 16.

Atwater, GSA Bull. 1970

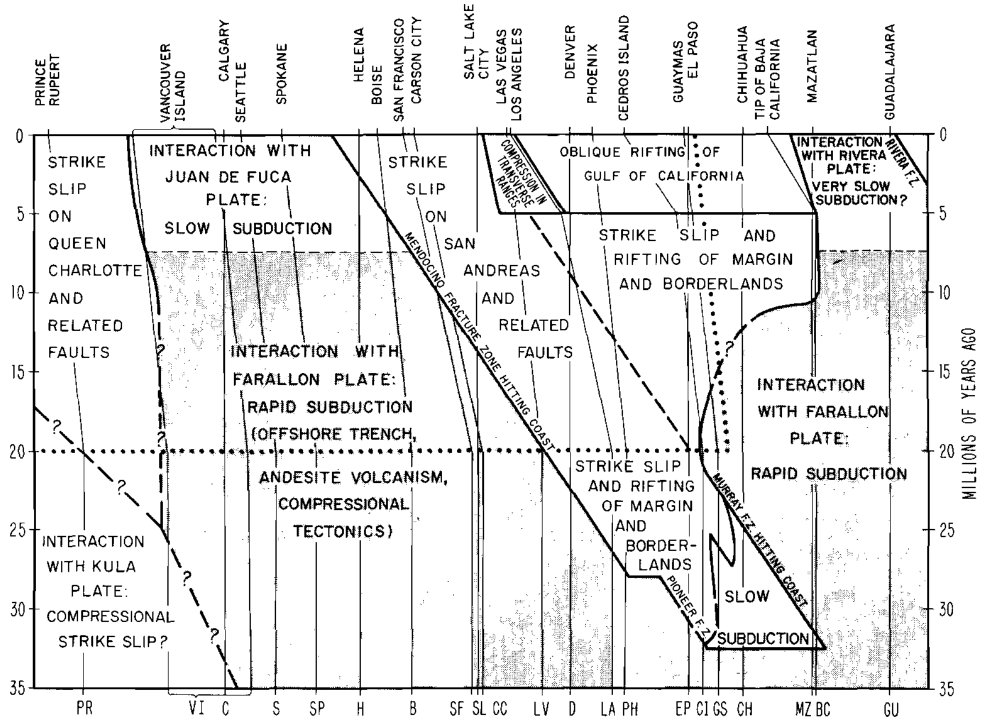

Figure 17. Location of plate boundary regimes with respect to points in western North America, assuming motions and deformations described for Figure 16. Inland cities are raised above the line. They have been projected to the coast vertically in the projection of Figure 16, roughly parallel to the direction of Farallon-North American underthrusting. Fine lines trace the shifting locations of the cities as the continent deforms. Gray areas show times and places where tectonic and igneous activity related to subduction are predicted. White areas show times and places where North America was in contact with the Pacific plate (or with the Kula plate, to be discussed below). The probable near-coast manifestations of these interactions are stated. The dotted line encloses the time and space included in the inland deformation zone of Figure 16. Although it is part of the North American-Pacific interaction, this zone overlaps the Farallon-Pacific field, so that effects of the 2 regimes may be superimposed. For example, around Carson City, andesite volcanism is predicted through the middle Tertiary until 11 m.y. ago, while strike-slip and basin-range rifting is predicted to have started 20 m.y. ago, lasting to the present day.

Atwater, GSA Bull. 1970

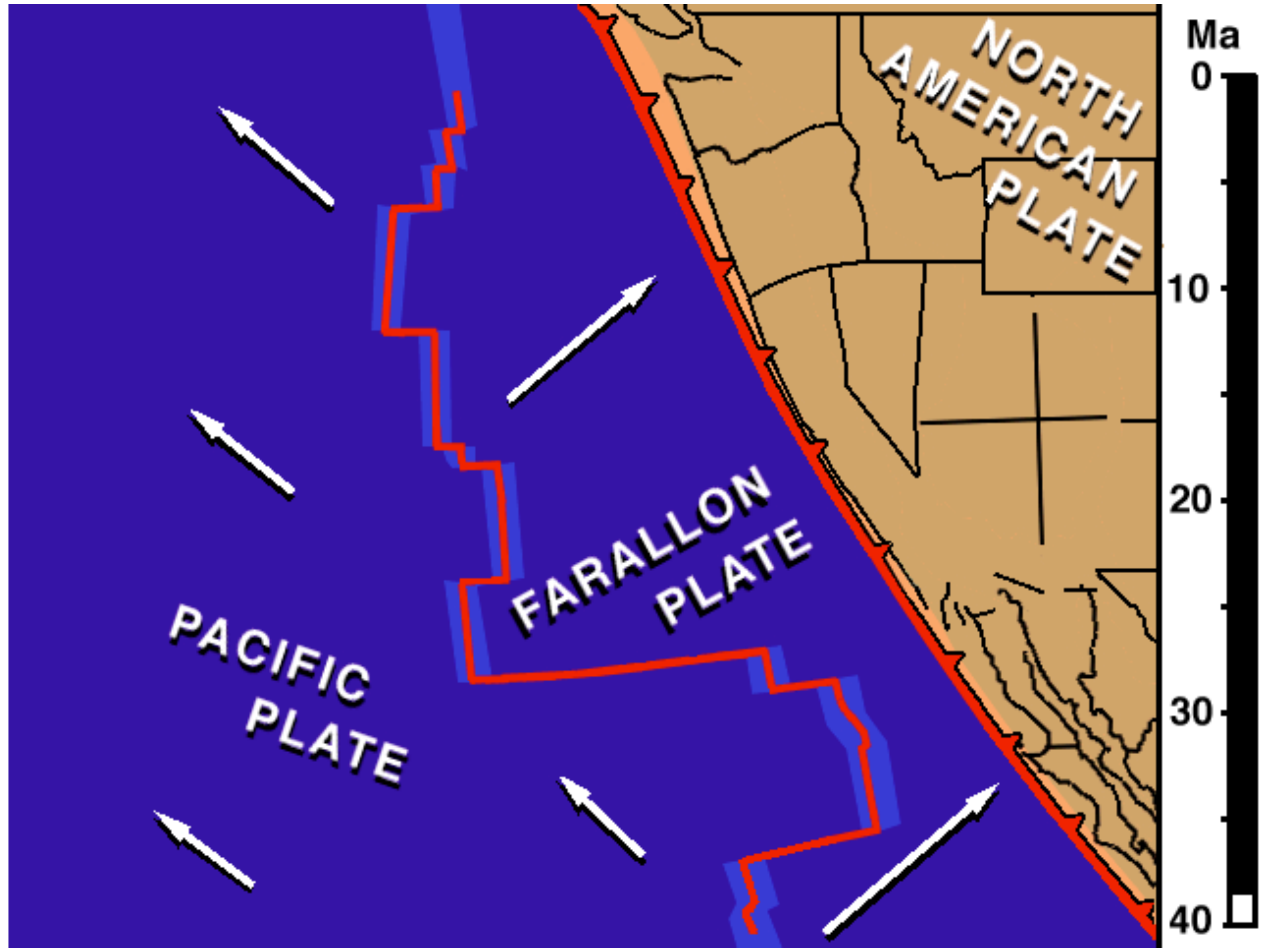

T.Atwater animation

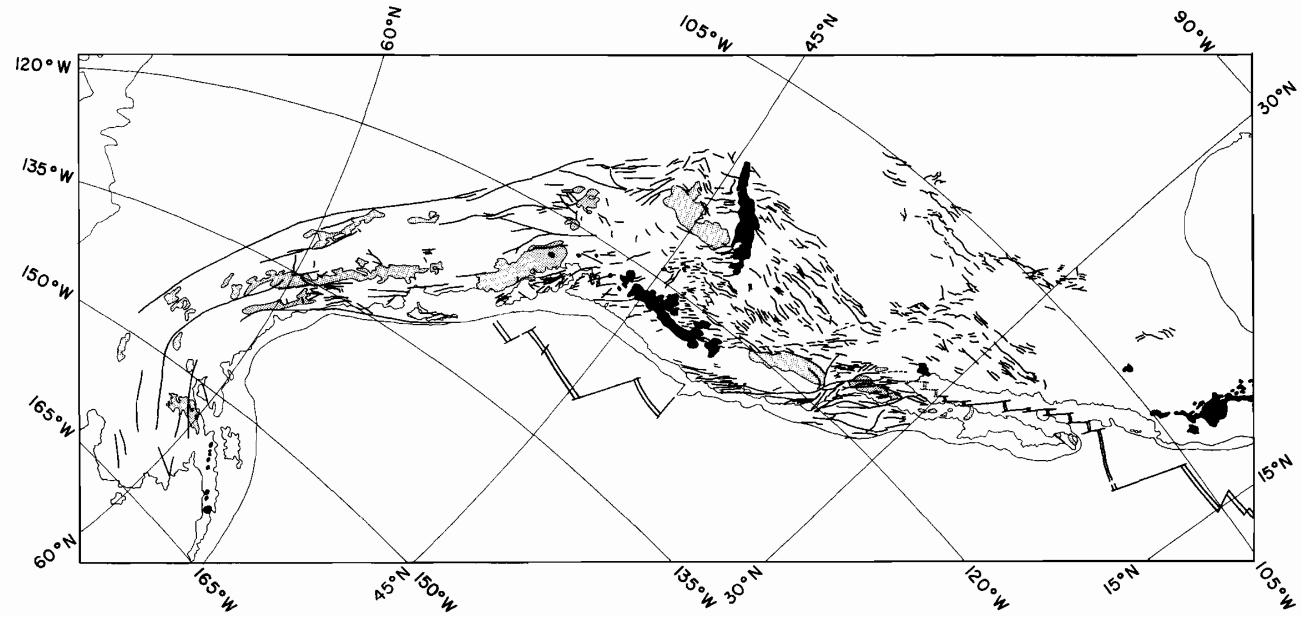

Figure 14. Some major tectonic features of western North America (*after* King, 1969). Quaternary volcanic rocks are black; granitic plutonic rocks are gray; most thrust faults have been omitted. Map projection is that used in Figure 4, so that deformation related to the motion between the American and Pacific plates can be imagined by keeping the ocean floor rigid and moving the rigid part of North America horizontally to the right. Horizontal faults experience pure strike slip while oblique faults have components of rifting or compression. A large-scale version of this projection is available from the author.

Atwater, GSA Bull. 1970

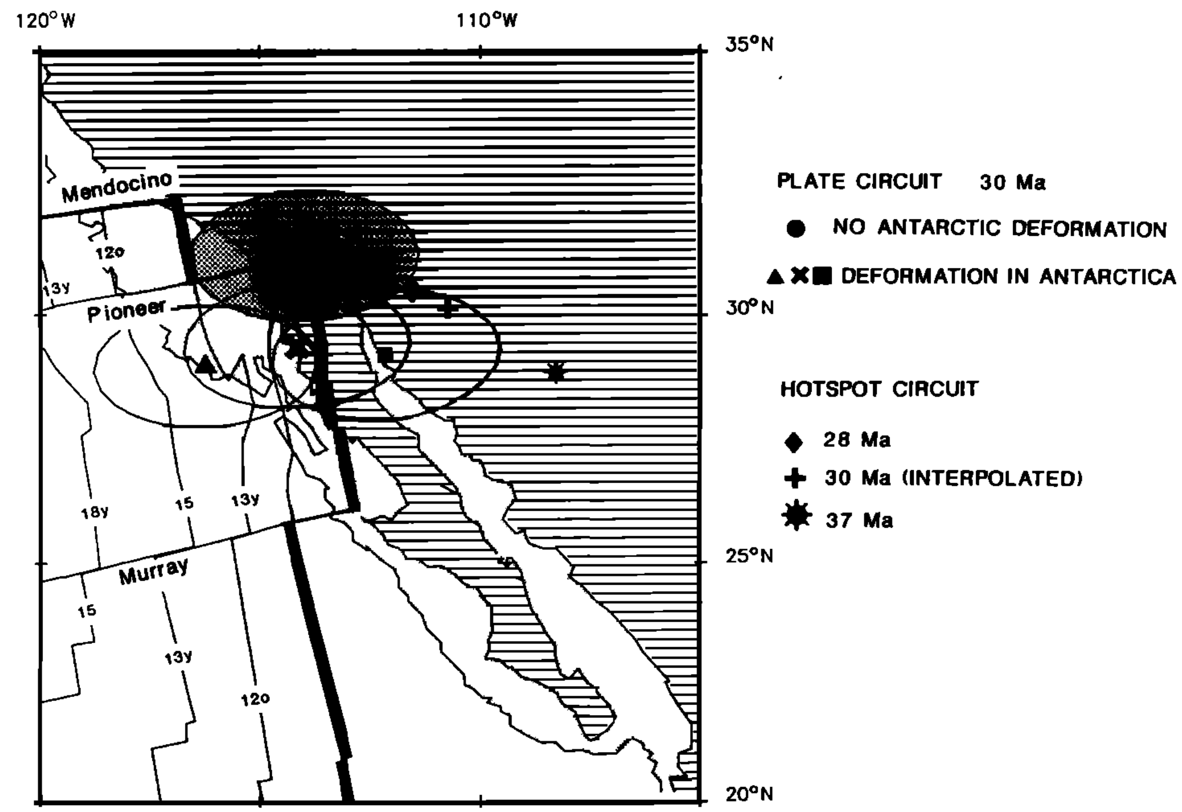

Stock and Molnar, Tectonics 1988

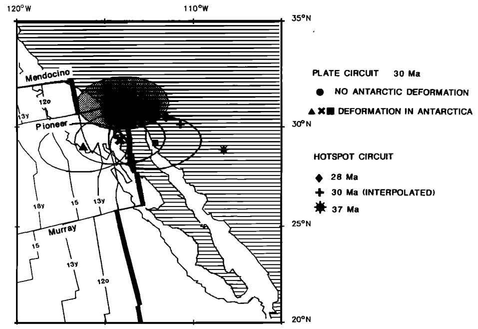

Stock and Molnar, Tectonics 1988

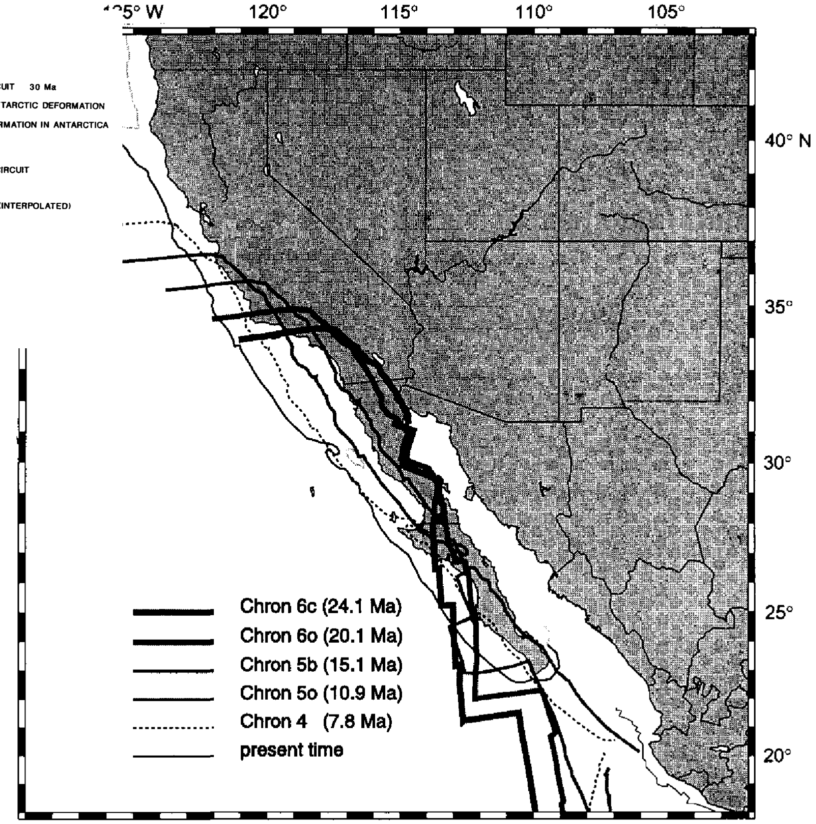

FIG. 5. Successive locations of the eastern edge of Pacific plate oceanic lithosphere, relative to a fixed North America, plotted upon the present shape of North America. The edge for each time step was drawn as described for Figure 4. The overlaps demonstrate the amount of internal deformation required within North America at each past time in order to avoid an unacceptable overlap of oceanic and continental lithosphere.

Atwater, & Stock, Intl Geol Rev. 1998

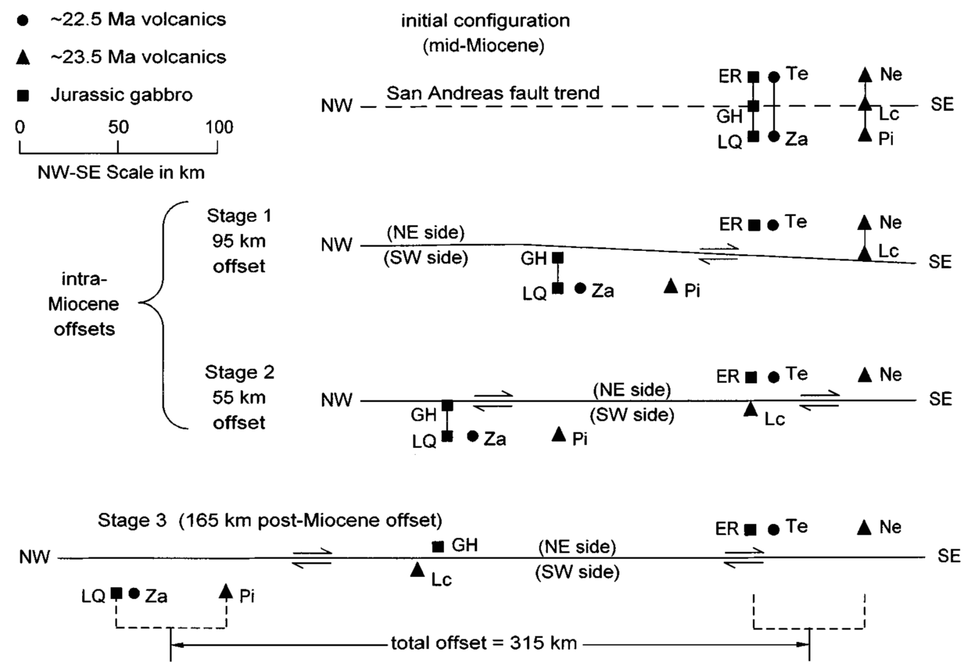

Figure 4. Diagram illustrating sequential fault offsets along San Andreas strands in central California required to reconcile present outcrop distribution of (1) Jurassic gabbro (ER, Eagle Rest Peak in San Emigdio Mountains; GH, Gold Hill beside Cholame Valley; LQ, Logan quarry near San Juan Bautista); (2) approximately 22.5 Ma Zayante (Za) and Tecuya (Te) formations (Table 1); and (3) approximately 23.5 Ma Pinnacles (Pi), Lang Canyon (Lc), and Neenach (Ne) volcanics (Table 1). Key information is from Sims (1993). Northeast-southwest scale is schematic.

Dickinson, GSA Bull 1997

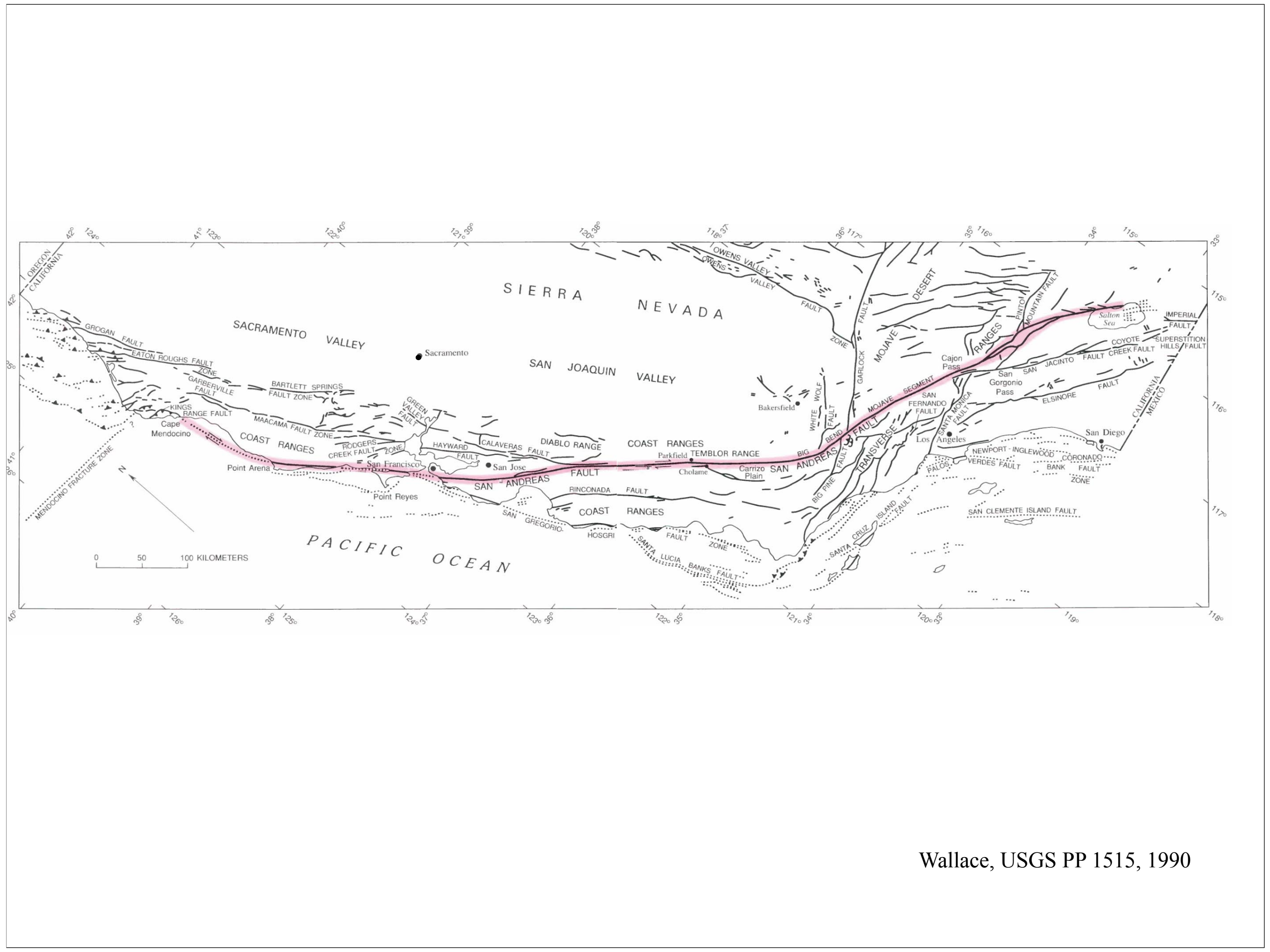

Note inboard movement of SAF with time/distance south.

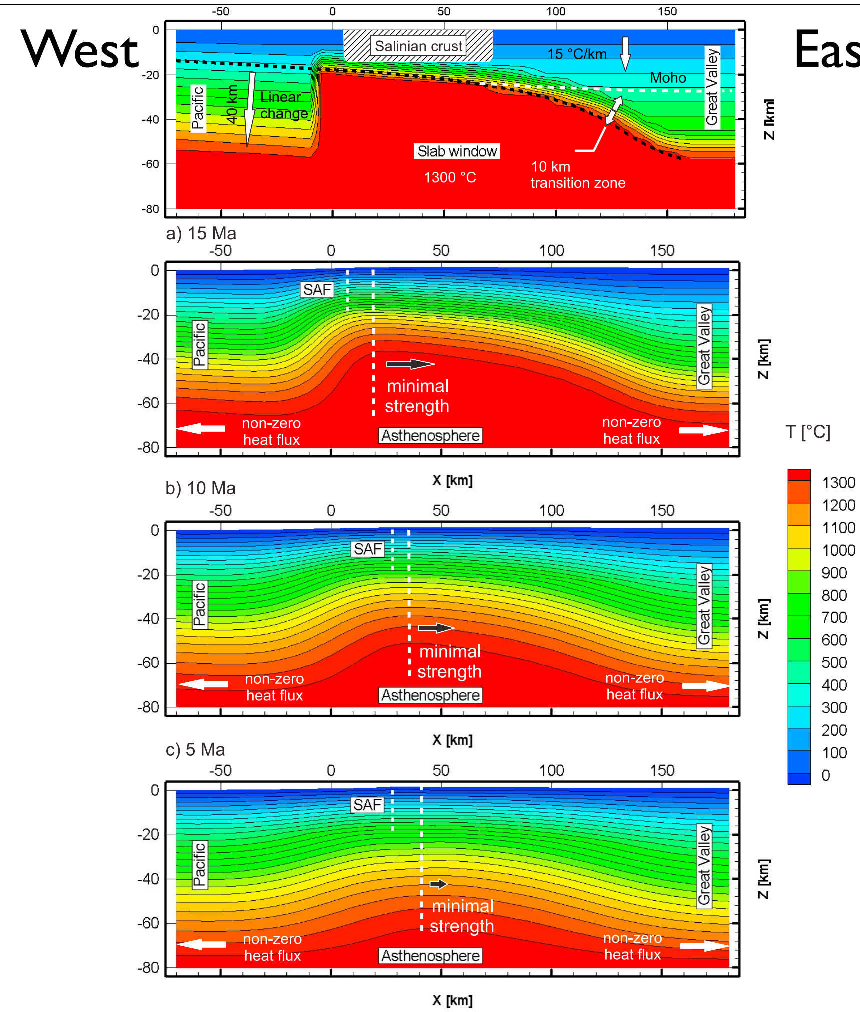

SAF to east by cooling of slab window?

Popov et al., G^3, 2013

Is this evolution of the slab window?--Authors think not, arguing that shear heating in mantle [is this a process we have any evidence of?], asthenospheric upwelling [which is model dependent--and in a 2013 paper to rely on the Benz tomography, which cannot extract mantle from crust--is disingeneous]

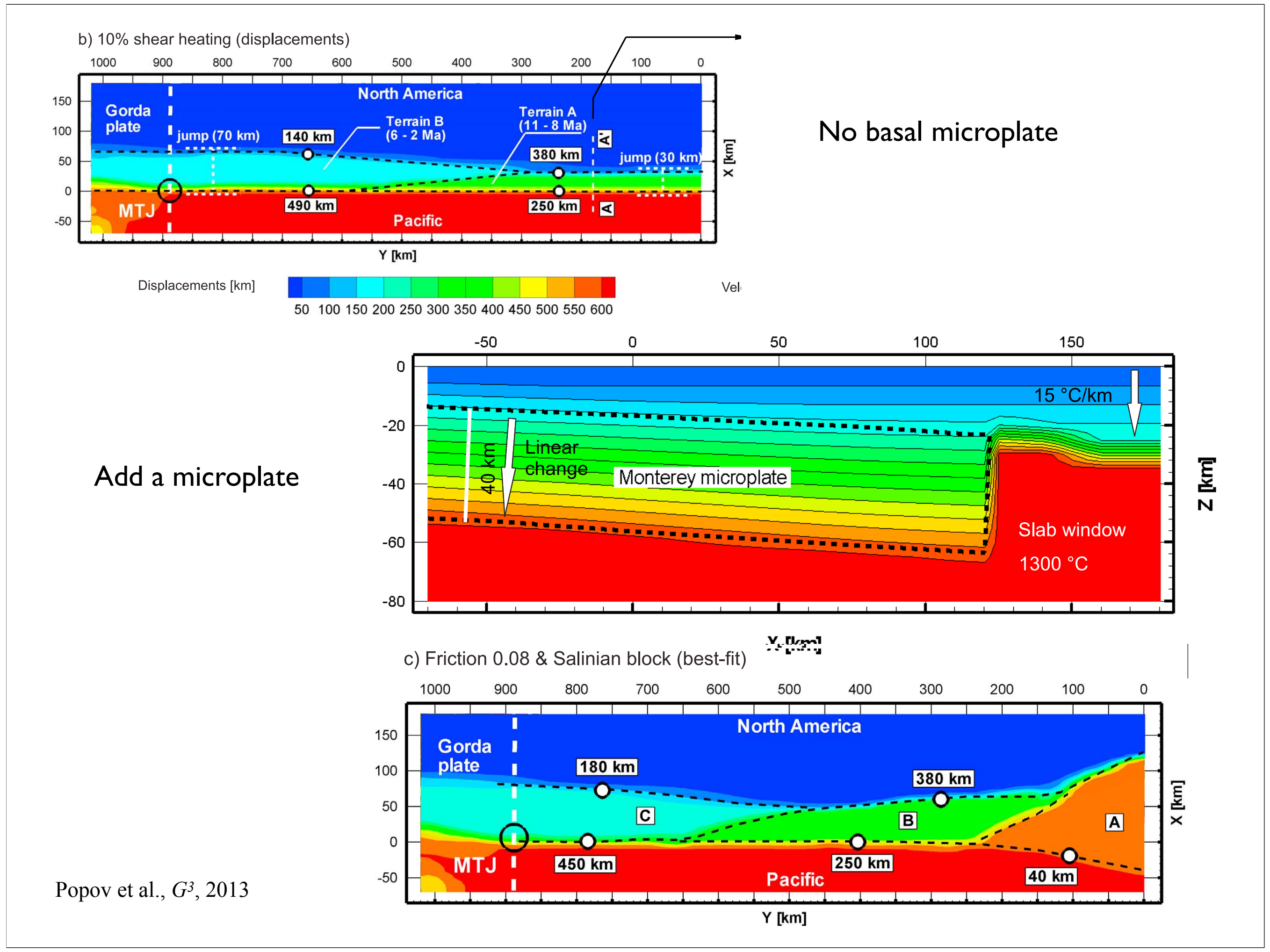

Generally this paper wants to argue for weak faults and strong plates. Kind of wonder if thermal structure of Monterey microplate is correct.

Top: Influence of 10% shear heating on the terrane accretion. Shown are the total strike-slip displacements (colors) on the top boundary of the model. Note different meaning of color on the top views and in the profiles. Also shown are the accumulated slips on the faults (white circles with labels), terrane widths, and accretion time spans.

Middle: Initial simplified thermal and crustal structure of the model. Colors indicate temperature magnitudes in C. The uniform initial temperature gradient 15C/km is assumed. Temperature distribution in the oceanic slabs is linear along the slab thickness. The 10 km transition zone is imposed between the top of the Gorda slab and the slab window. (c) Temperature profile in the Monterey microplate (profile C–C′).

Bottom: Influence of the microplate and strong crustal block on the terrane accretion. Shown are the total strike-slip displacements (colors) on the top boundary of the model. Distinct terranes are labeled with letters. White circles with labels indicate accumulated slips. The faults are marked with dashed lines. Results of the model with crustal block and saturated friction 0.08 (reference model).

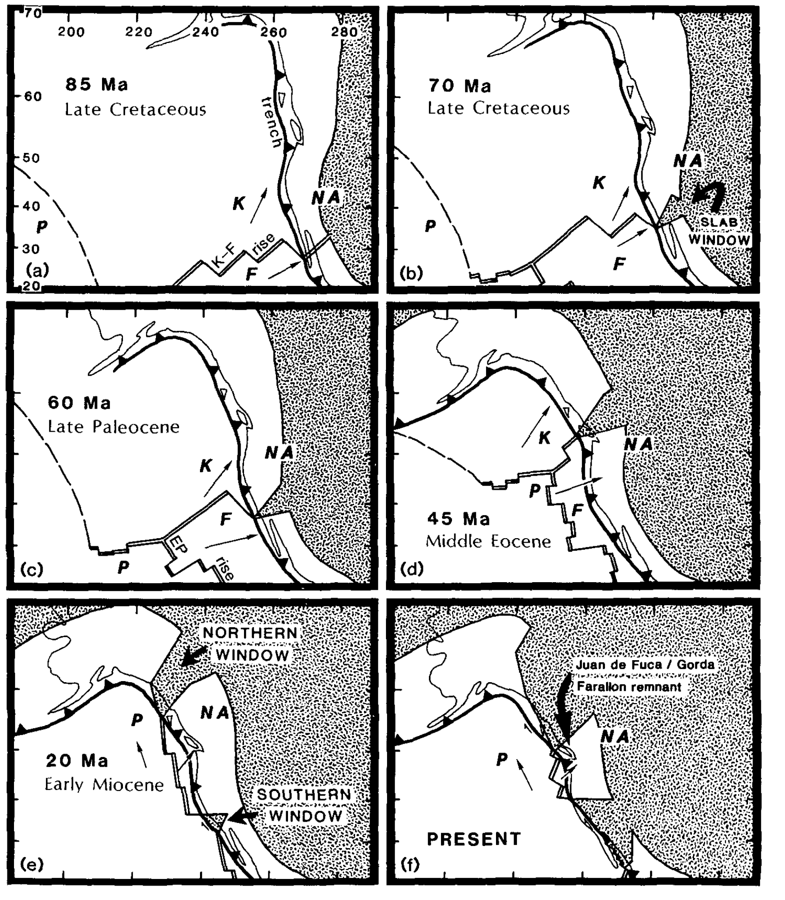

Figure 1. Slab windows beneath North American Cordillera from Late Cretaceous to present, based on plate reconstructions by Riddihough (1982), Engebretson et al. (1985), Lonsdale (1988), and Stock and Molnar (1988). Stippled pattern identifies areas where asthenospheric mantle would have directly underlain North American plate, based on 100 km maximum thickness for continental lithosphere and subduction angle of 5°. Plate motion vectors relative to "fixed" North America, shown for periods of 10 m.y. (Engebretson et al., 1985; Lonsdale, 1988; Stock and Molnar, 1988), were used to construct window shapes. Latitude and longitude, as labeled in a, are same in all diagrams. Southern Pacific–Farallon slab window, shown in e and f, was previously illustrated by Dickinson and Snyder (1979). Plates: F = Farallon; K = Kula; NA = North American; P = Pacific; EP = East Pacific.

Thorkelson & Taylor, Geology 1989

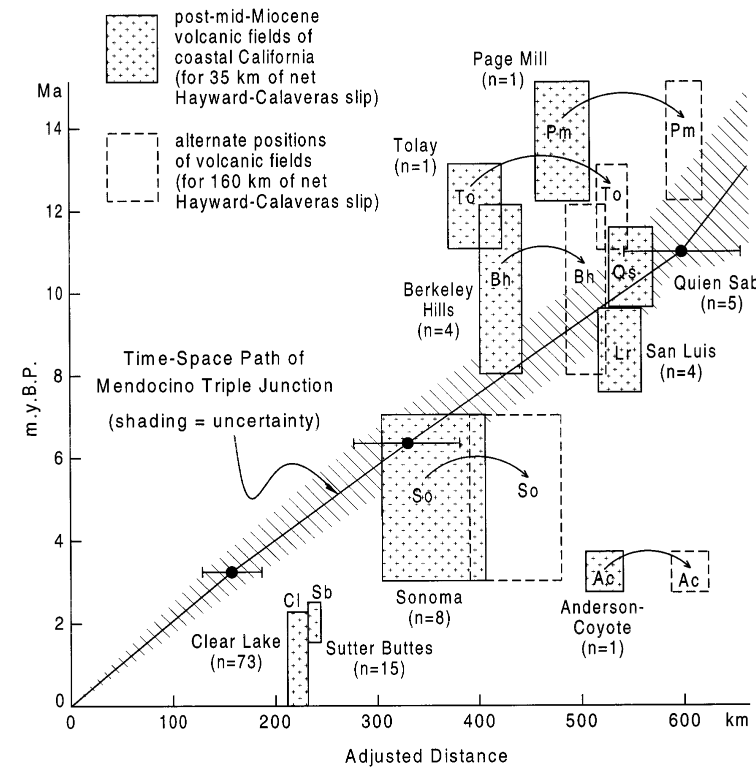

Figure 9. Time-distance plot (adapted and updated after Fox et al., 1985, and Atwater, 1989) of the Mendocino triple junction (shaded) and post–mid-Miocene volcanic fields (stippled) in coastal California (data from Table 3). Adjusted distance is the distance along the San Andreas transform trend from the present position of the Mendocino triple junction. The temporal-spatial correlation of ages of volcanics with the triple junction path (as shown) required adjustment of positions of volcanic fields to allow for tectonic transport (approximately 57.5 km) across eastern California shear zone (of Dokka and Travis, 1990), as well as slip along splay faults of San Andreas system in the San Francisco Bay area. Dashed positions of selected fields are plotted for the alternative of large displacement along the Hayward-Calaveras splay fault system (after McLaughlin et al., 1996); curved connecting arrows show relationships to alternate positions (stippled) plotted for the assumption of lesser displacement (after Graham et al., 1984).

Dickinson, GSA Bull 1997

Second phase is migration of slab-free window with triple junction

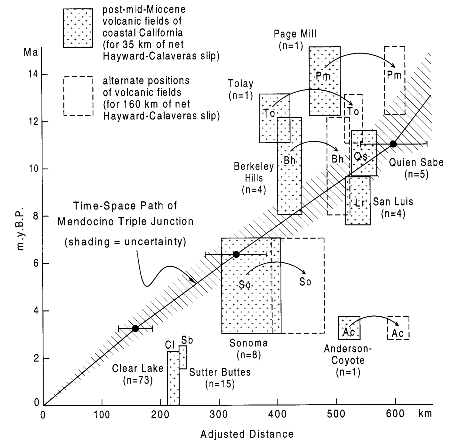

Figure 9. Time-distance plot (adapted and updated after Fox et al., 1985, and Atwater, 1989) of the Mendocino triple junction (shaded) and post–mid-Miocene volcanic fields (stippled) in coastal California (data from Table 3). Adjusted distance is the distance along the San Andreas transform trend from the present position of the Mendocino triple junction. The temporal-spatial correlation of ages of volcanics with the triple junction path (as shown) required adjustment of positions of volcanic fields to allow for tectonic transport (approximately 57.5 km) across eastern California shear zone (of Dokka and Travis, 1990), as well as slip along splay faults of San Andreas system in the San Francisco Bay area. Dashed positions of selected fields are plotted for the alternative of large displacement along the Hayward-Calaveras splay fault system (after McLaughlin et al., 1996); curved connecting arrows show relationships to alternate positions (stippled) plotted for the assumption of lesser displacement (after Graham et al., 1984).

Dickinson, GSA Bull 1997

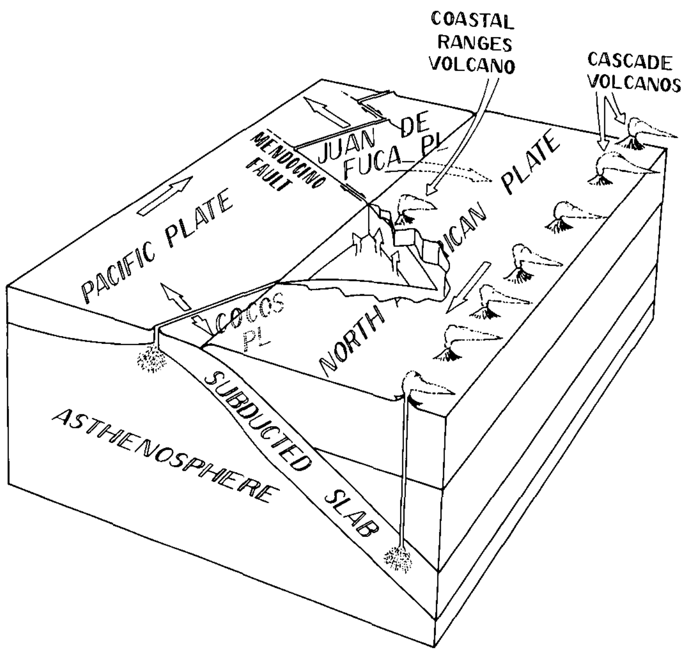

Figure 5. Block diagram showing plate geometry of northern Coastal Ranges volcanic rocks at ~20 Ma. Cutaways are for visualization only. Dotted arrow dipping beneath North American plate shows direction of movement of Farallon (and Juan de Fuca) plate with respect to North American plate. Subsequent telescoping of volcanic rocks along strike-slip faults is not shown, nor is the inferred change in spreading direction of the Juan de Fuca plate.

Fox Jr., et al., Geology 1985

Of course southernmost possible extent of Cascade volcanoes is Sonora Pass

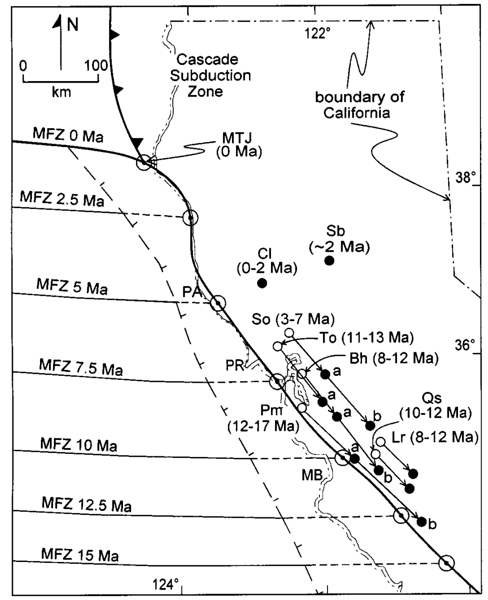

Figure 8. Reconstructed post–mid-Miocene positions of the Mendocino Fracture Zone (MFZ) and associated Mendocino triple junction (MTJ) offshore from central and northern California (after Dickinson, 1996) in relation to positions and ages of post–mid-Miocene volcanic fields (circles) in adjacent coastal California (from Figs. 1 and 2 and Table 3; Ac [Anderson-Coyote basalt] of anomalous age not plotted). Positions of >5 Ma volcanic fields are restored (solid circles) for 55–60 km of dextral shear (parallel to San Andreas fault trend) along eastern California shear zone after Dickinson (1996), and alternately for (a) 35 km of dextral strike slip along the Hayward-Calaveras fault zone (apportioned equally to each branch after Graham et al., 1984), and (b) 160 km of Hayward-Calaveras slip apportioned 60 km to Hayward fault zone and 100 km to Calaveras fault zone (after McLaughlin et al., 1996). Hachured line offshore is approximate base of modern continental slope. Frame of reference is provided by present positions of Mendocino triple junction and boundary of California.

Dickinson, GSA Bull 1997

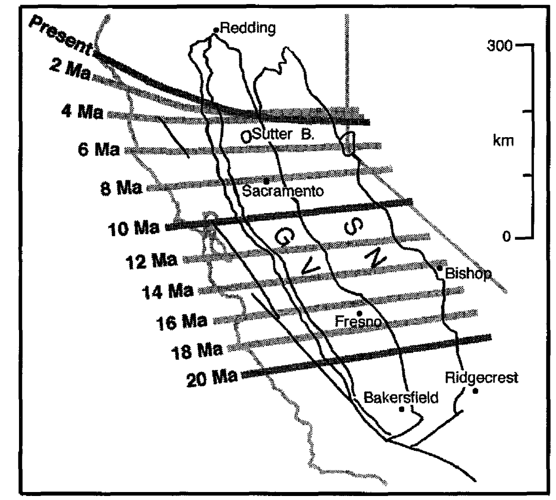

FIG. 11. Placement of the Mendocino edge of the subducting Juan de Fuca plate beneath the Sierran-Great Valley block, from 20 Ma to present. Drift of oceanic plates is interpolated from our circuit solutions; displacement of the Sierran-Great Valley block is drawn following Wernicke and Snow (1998); the shape of the Mendocino edges from 6 to 0 Ma is from Wilson (1989). Light grey coastline and state boundaries are given in their present-day locations for orientation purposes only.

Atwater & Stock, Int. Geol. Rev., 1998

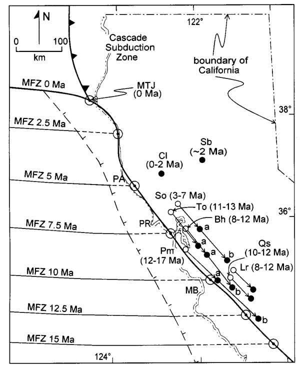

Dickinson, GSA Bull 1997

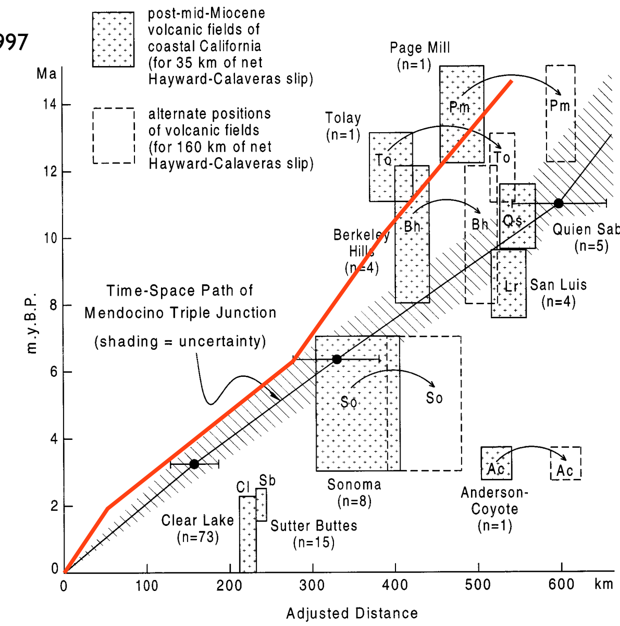

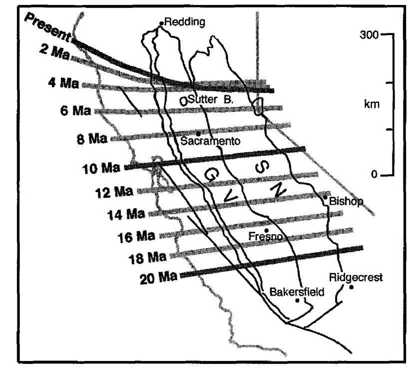

Atwater & Stock, Int. Geol. Rev., 1998

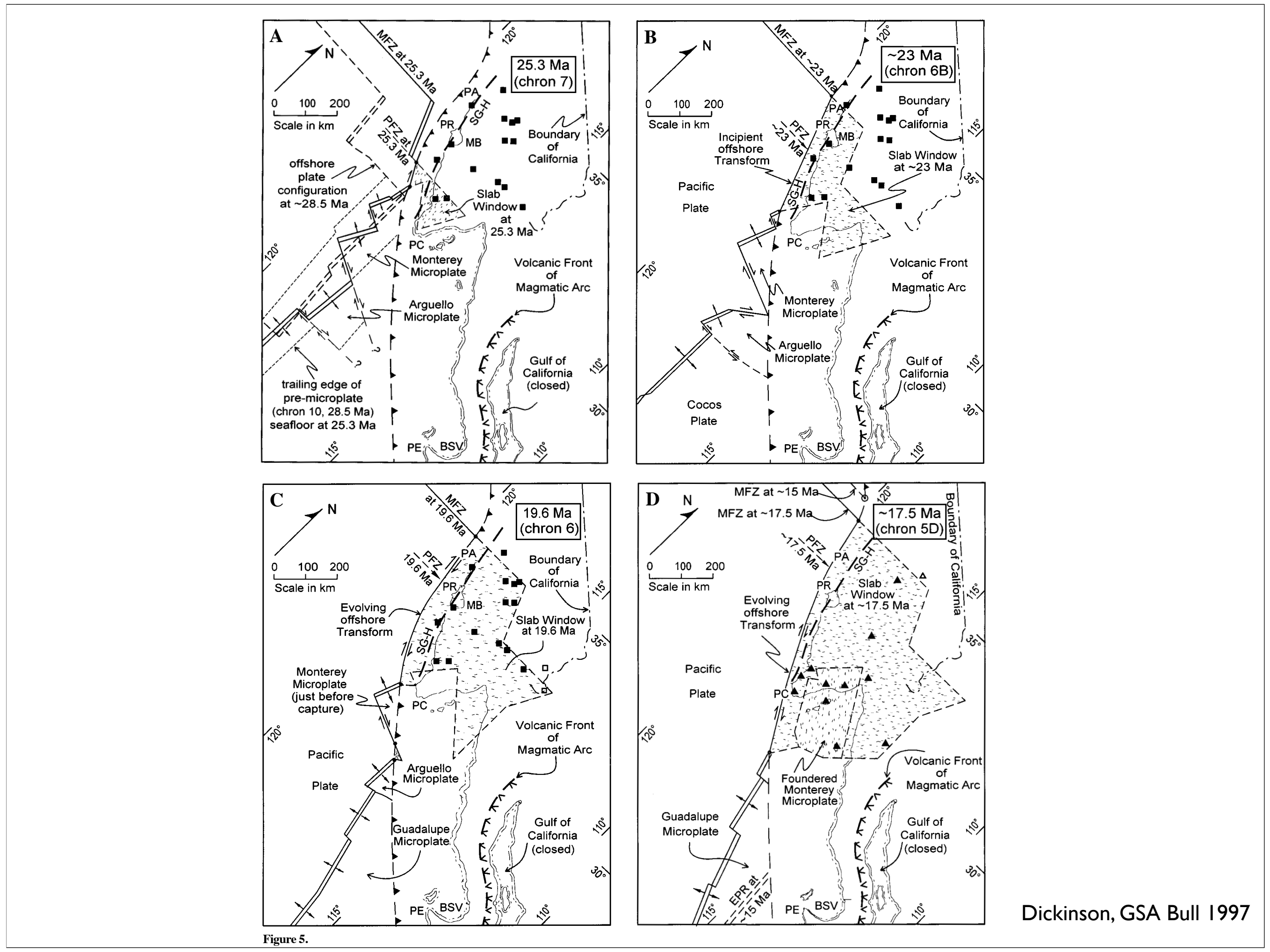

First stage of slab window is behind trench-ridge collision. Note that Dickinson foundered the Monterey microplate to get volcanism on top

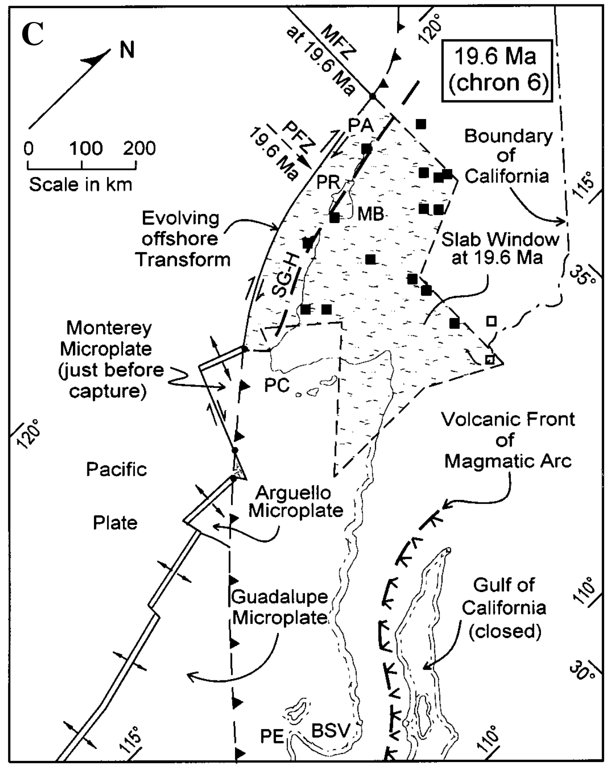

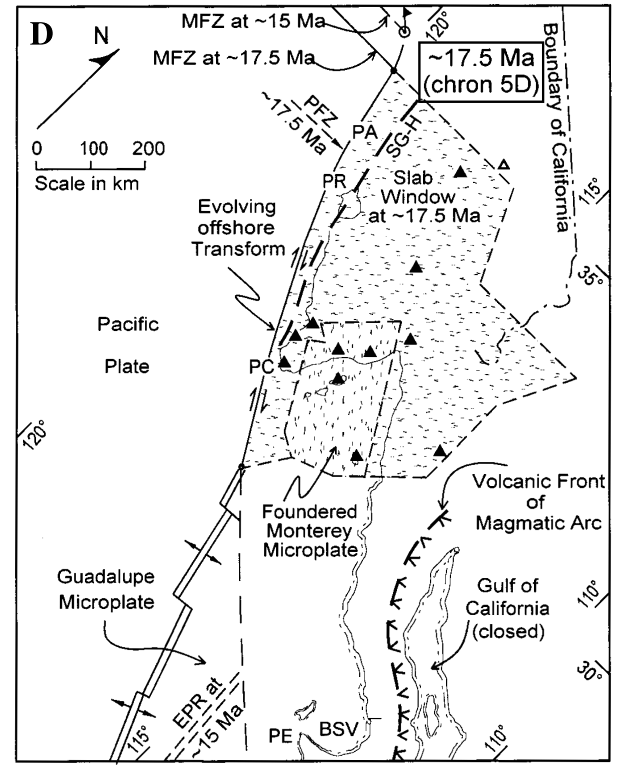

Dickinson, GSA Bull 1997

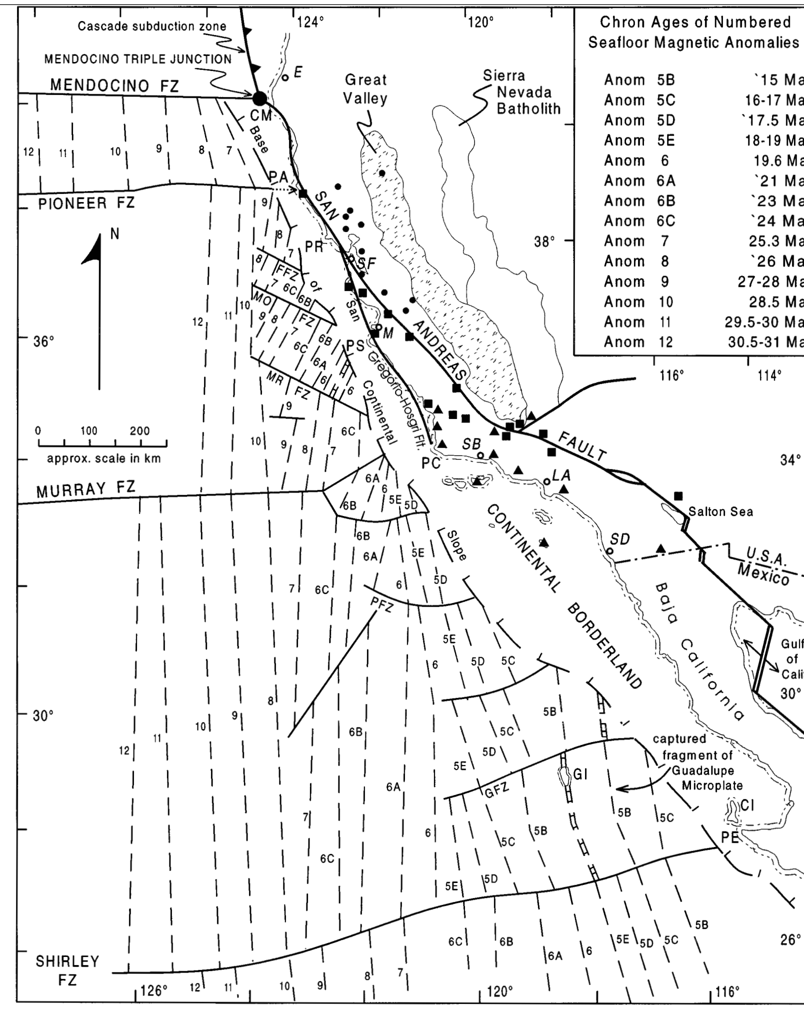

Dickinson, GSA Bull 1997

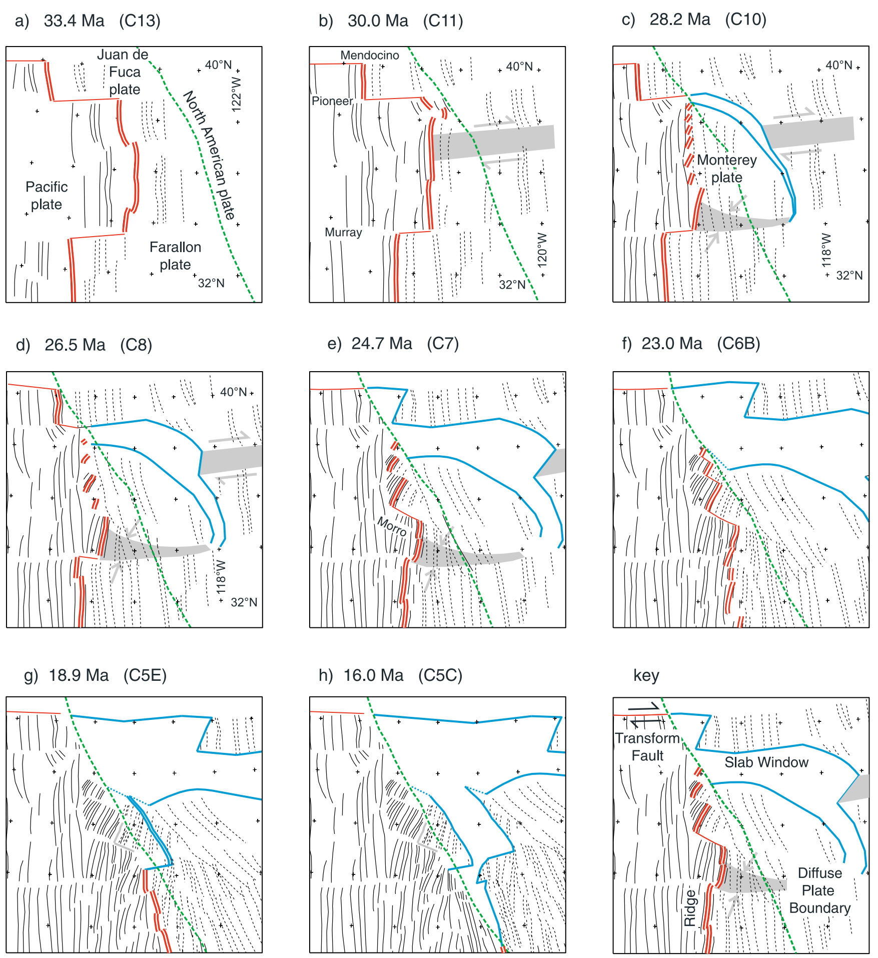

Wilson et al., *Tectonics*, 2005

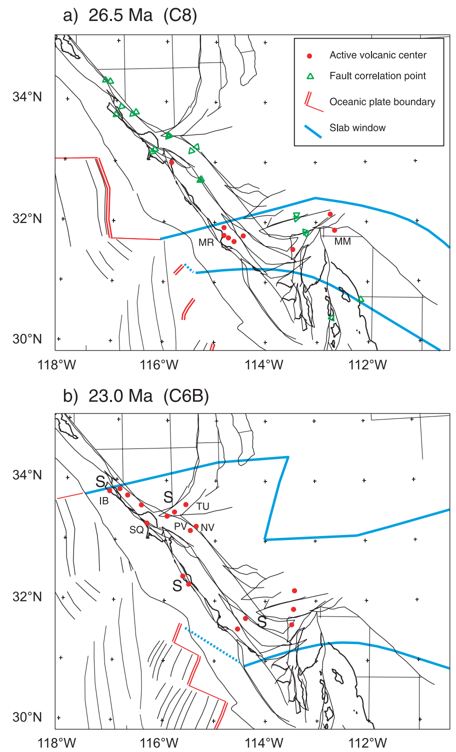

Figure 7. Reconstruction model showing positions of mid-Tertiary volcanic rocks relative to evolving slab windows north of the Monterey plate. (a) The 26.5 Ma (C8) reconstruction shows positions of 27–26 Ma volcanic centers, (b) 23.0 Ma (C6B) reconstruction shows positions of 24–22 Ma volcanic centers. With the exception of the Carmel area volcanic rocks, all volcanic centers can be restored to the slab window at their time of initial eruption. Slab windows are from Figures 3d and 3f but in North America fixed coordinates. "S" indicates a basin analyzed in Figure 9 showing rapid subsidence; triangles are fault correlation points from Figure 4.

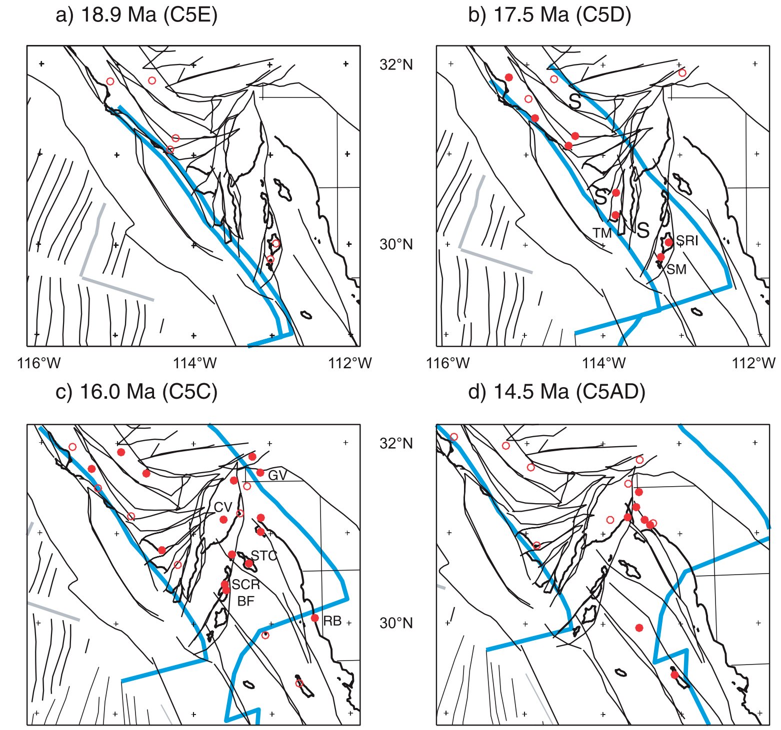

Figure 8. Reconstructions of 19–14 Ma volcanic centers compared with a slab window model east of the captured Monterey plate. Within each frame, volcanic centers with preferred dates at the reconstruction time or less than 1.5 Myr prior to it are plotted as solid circles; other volcanic centers with age uncertainties encompassing the reconstruction time are plotted as open circles. Other symbols are as in Figure 7. The initial position of the break at 19.1 Ma between the captured Monterey plate, and its slab is not known independently, but is assumed to lie west of the older volcanic rocks, near the Hosgri fault. The subsequent evolution of the slab window geometry (bold lines) is assumed to be governed by Cocos-Pacific relative plate motions. Within dating uncertainties, all volcanic centers except JV east of the map edge can be restored to above the slab window at their time of initial eruption. North America fixed coordinates.

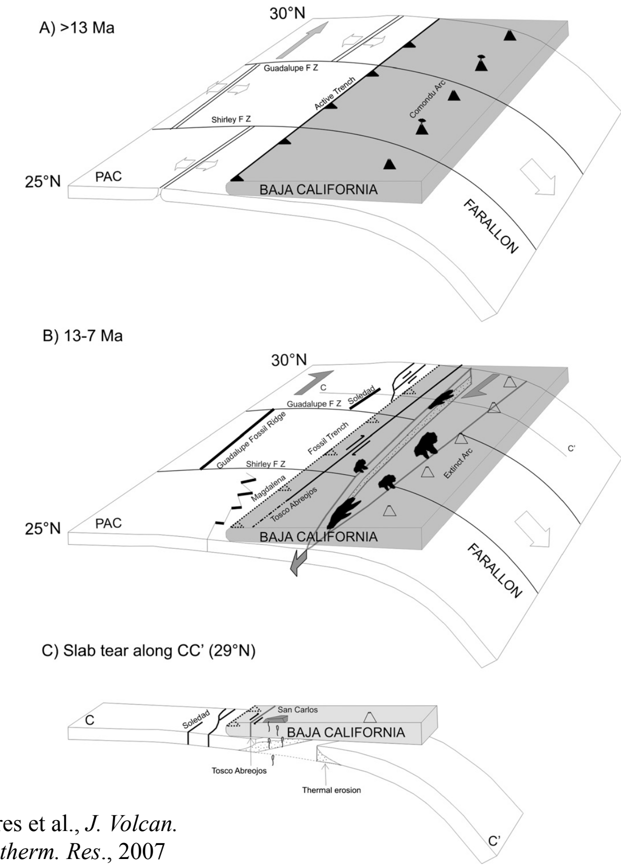

Pallares et al., *J. Volcan. Geotherm. Res.*, 2007

Fig. 6. Proposed schematic model of slab-tearing prior to ridge-trench collision. The upper plate (shaded) is shown with dotted lines, the downgoing plate (white) with plain lines, arc volcanoes (upper cartoon) and basaltic plateau flows (middle cartoon) in black. Scale and main structural elements are as in Fig. 2. Stage A (>13 Ma): active subduction and edification of the Comondú arc. Stage B (13–7 Ma): end of subduction and development of a slab tear which evolves into a slab window, post-subduction magmatism. The trench becomes fossil and the Tosco–Abreojos dextral strike-slip fault propagates southward. The tear is represented at an early stage of development, when thermal erosion (stippled areas) starts to reduce the thickness of its lithospheric edges. C: schematic cross-section along line CC' (in B), at ca. 29°N, depicting the effects of thermal erosion and the ascent of infraslab magmas (San Carlos alkali trachybasalts) through the tear.

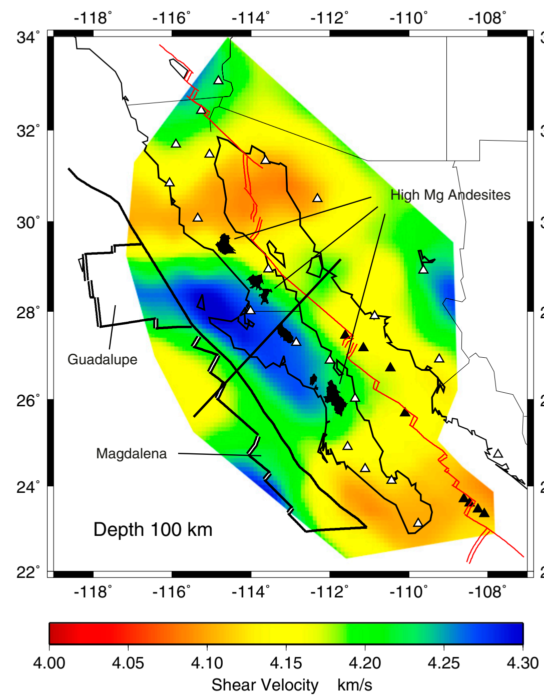

Wang et al, *PNAS*, 2013

This is in some ways similar to argument of Popov paper as this makes it easier to grab Baja to move northward

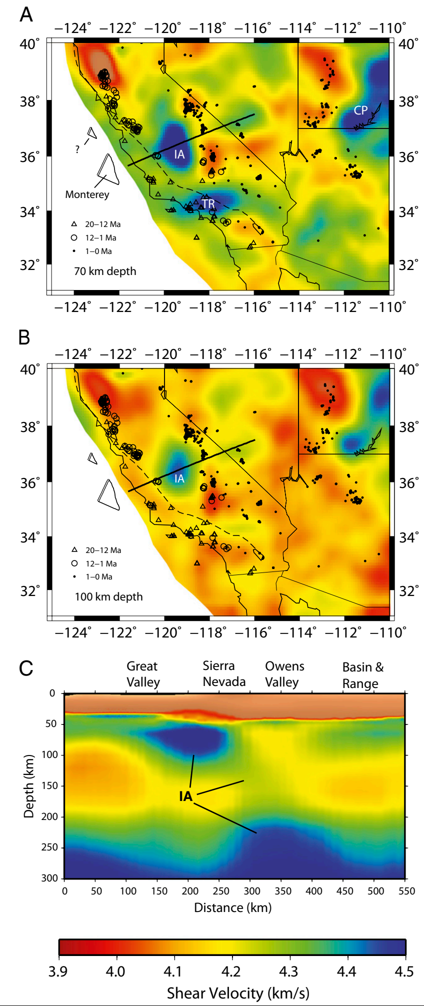

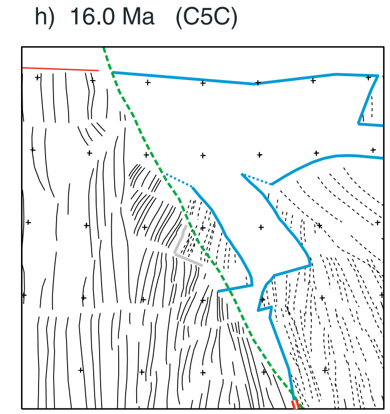

Wilson et al., *Tectonics*, 2005

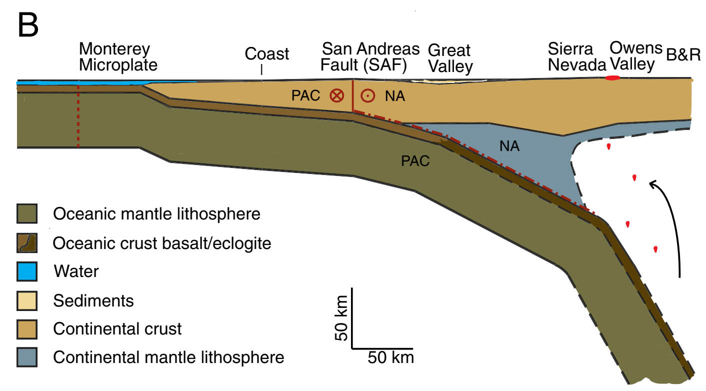

Wang et al, *PNAS*, 2013

Extreme micoplate--holding on to Monterey microplate (last spreading anomaly 6--19 Ma). but it is NORTH of where Monterey plate last was

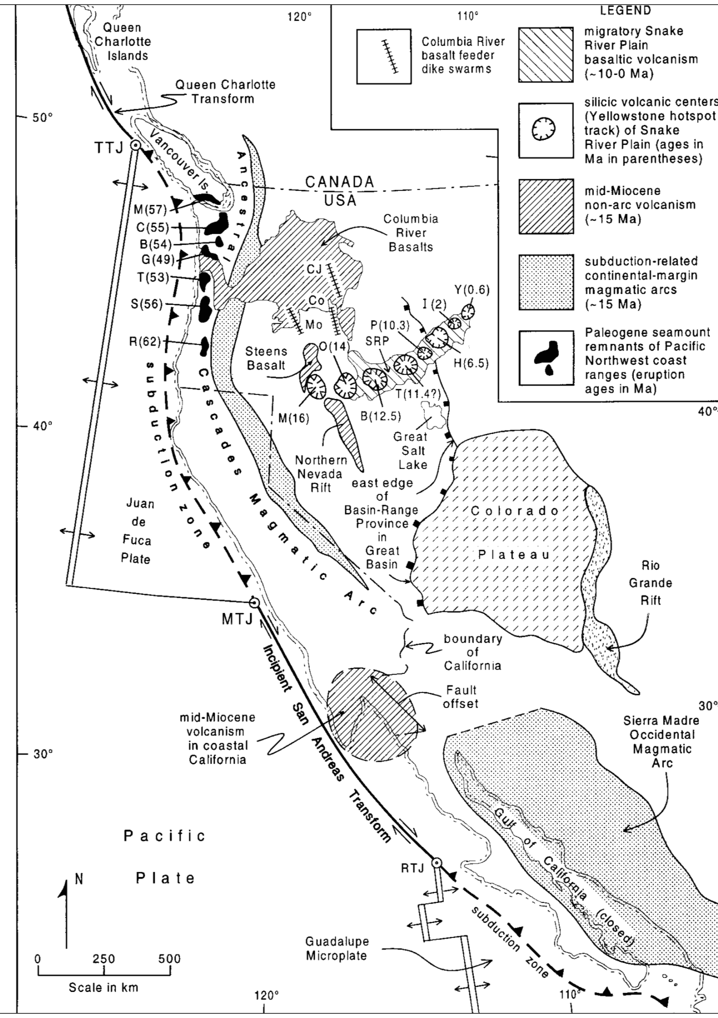

Dickinson, GSA Bull 1997